Large-Scale Synthesis of Nanosilica from Silica Sand for Plant Stimulant Applications

Cao Van Hoang,* Dang Nguyen Thoai, Nguyen Thi Dieu Cam, Tran Thi Thu Phuong,
Nguyen Thi Lieu, Tran Thi Thu Hien, Dao Ngoc Nhiem, Thanh-Dong Pham, Mai Huynh Thanh Tung,
Nguyen Thi To Tran, Adam Mechler, and Quan V. Vo*

Read Online

ACCESS | Metrics & More | Article Recommendations | SI Supporting Information

ABSTRACT: Nanosilica is a versatile nanomaterial suitable as, e.g., drug carriers in medicine, fillers in polymers, and fertilizer/pesticide carriers and potentially a bioavailable source of silicon in agriculture. The enhanced biological activity of nanosilica over quartz sand has been noted before; it is directly related to the altered physicochemical properties of the nanoparticles compared to those of the bulk material. Therefore, it is feasible to use nanosilica as a form of plant stimulant. Nanosilica synthesis is a relatively cheap routine process on the laboratory scale; however, it is not easily scalable. Largely for this reason, studies of nanosilica fertilizers are scarce. This study will focus on industrial-scale silica nanoparticle production and the application of nanosilica as a plant stimulant in maize. A variant of the sol–gel method is used to successfully synthesize nanosilica particles starting from silica sand. The resulting particles are in the size range of 16–37 nm with great purity. The potential of nanosilica as a plant stimulant is demonstrated with the increased quantity and quality of maize crops.
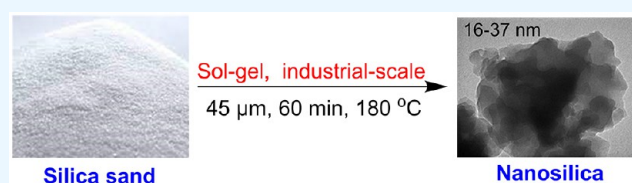
1. INTRODUCTION

SiO_2 nanoparticles have markedly different properties from those of naturally occurring quartz sand. With large effective surface area, often distinct mesoporosity, and easy functionalizability, they are good dynamic adsorbers and thus already widely used, for example, in medicine,[1] as drug carriers,[2] in polymers,[3–5] and as carriers of biologically active chemicals in agriculture.[6–9] Nanosilica is particularly useful in the realm of agriculture.[10,11] Plants rely on nanosilica for silicon because lignin production is influenced by silicon.[12] Silica is a nutrient that promotes growth, increases crop output, and improves the quality of agricultural goods by assisting in the formation and regeneration of plant cell walls.[13] Si deposition plays a similar role to that of lignin in the cell walls.[12] Under high transpiration, silicon prevents xylem layer compression.[14,15] It is frequently seen in experiments with nanosilica added to either the culture solution or the plant soil that the plants exhibit increased hardness and tenacity, making the plants stronger.[12,13,16–18] Experiments on rice have shown that it approached 30% in severe leaf blasts.[19] Liang and co-workers used Si to dramatically increase the development of cotton plants affected with root rot disease in another study.[20] In most crops, silicon plays a physiological role in decreasing biotic and abiotic stress.[19–26] Although the advantages and disadvantages of using nanomaterials as fertilizers are controversial from the consumer safety point of view,[7,27–30] there are numerous studies on using nanosilica for agriculture with positive effects on crops.[10,27,31,32] Therefore, it is required to develop a simple, scalable approach for the industrial manufacturing of nanosilica, while deferring the assessment of safety as a concern of licensing.

Chemical methods such as sol–gel or hydrothermal synthesis are frequently used to make amorphous silica nanoparticles of >95% purity from various precursors, including organic silica sources such as rice husk ash that has 85–98% silica content.[33–37] Sodium silicate solution, which is used to make silica nanoparticles, was made with silica sand in several studies.[6,32,38–44] Amorphous silica nanoparticles with a particle size of about 60 nm were obtained by following the alkali fusion route using NaOH at 500 °C.[38] Nanosilica was also produced from silica sand[44] with average particle sizes of 80 nm and 170 nm.[32] Three different processing techniques—sol–gel, sonication, and spray pyrolysis—were used to create silica nanoparticles from natural quartz sand, yielding a mesoporous material with an average size of 10–26 nm.[40] However, the scalability of the common nanosilica producing methods was not well developed. Most studies only made silica nanoparticles at the laboratory scale with a broad size range of nanomaterials that is not suitable for the industrial production of fertilizers, whereas little attention was paid to finding a simple scalable method suitable for industrial nanosilica
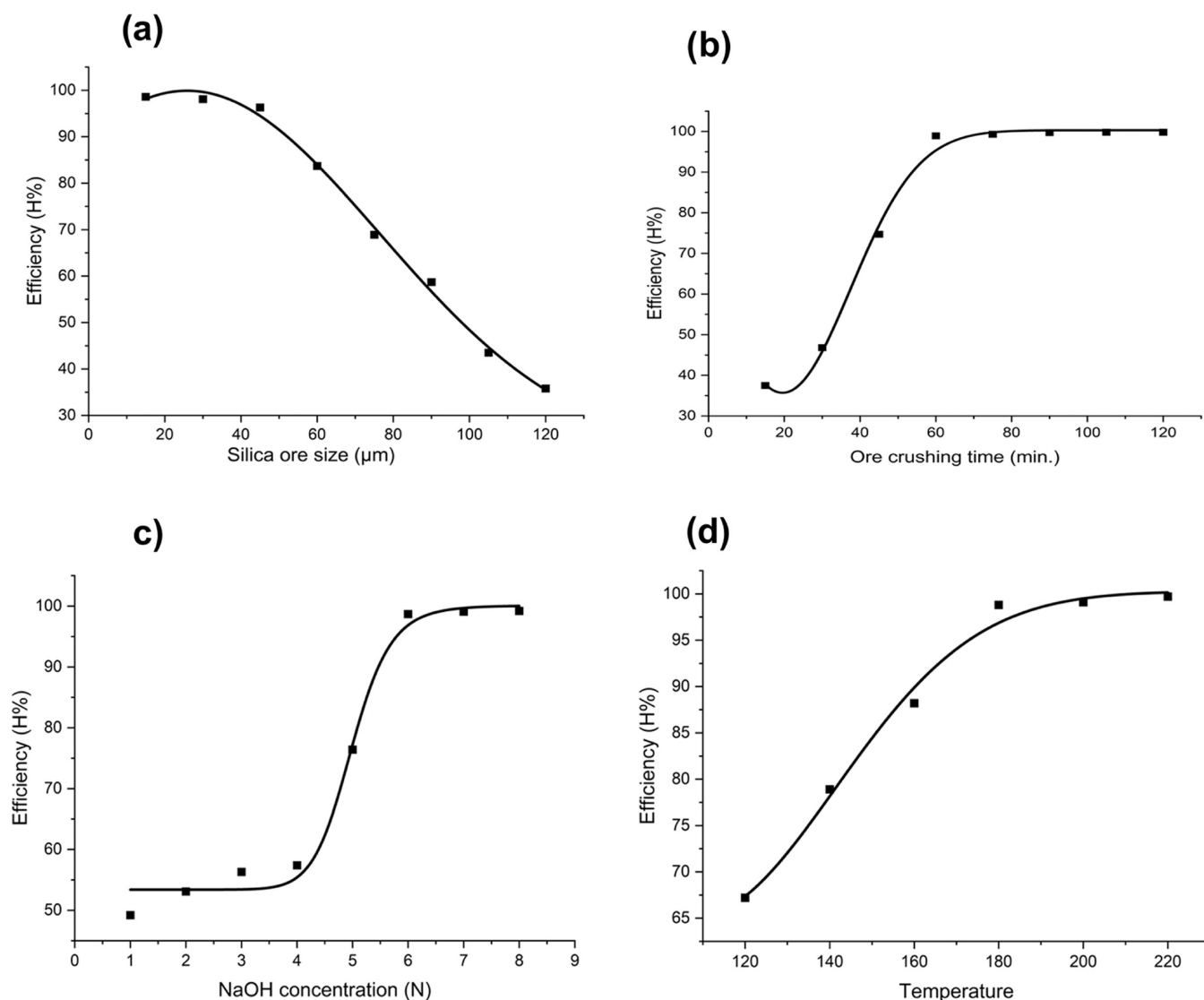
Figure 1. Effects of experimental conditions on the efficiency: (a) silica ore size; (b) crushing time; (c) NaOH concentration; and (d) temperature (°C).

production. The central aim of this work is optimizing industrial-scale silica nanoparticle synthesis starting from sand and a case study of application as a plant stimulant in maize.

2. RESULTS AND DISCUSSION

2.1. Optimization of Conditions. It is known that the particle size of the starting material has a great influence on the ability of NaOH solution to dissolve silica.[45,46] Thus, the precursor silica particle size and NaOH concentration are optimized first. The results are presented in Figure 1.

As shown in Figure 1a, the dissolution efficiency of SiO_2 in the 60 min timeframe (180 °C) reached a plateau at <50 μm sizes. Improved dissolution kinetics with decreased size were directly related to the exposed surface area, as the optimum size was too large for any effect of size-related changes in surface chemistry. Under the studied conditions, when crushing the sand to 15 μm, the energy consumption was 10 times higher than that under crushing to 45 μm size for no appreciable improvement. Thus, the particle size of 45 μm was chosen for further studies. For the investigation of the effect of
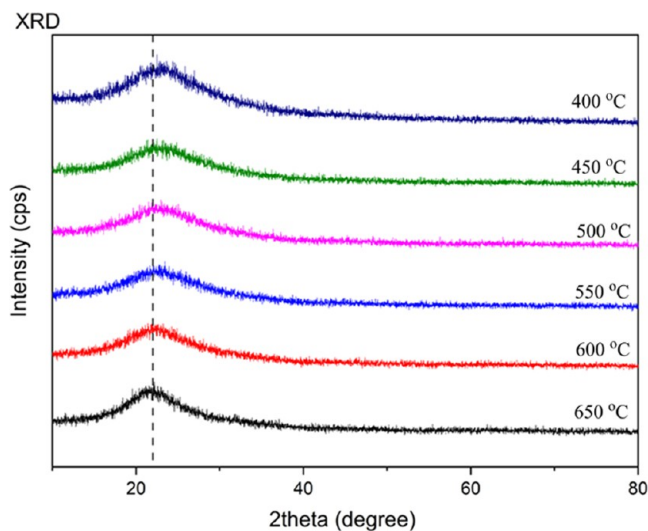

Figure 2. XRD pattern of nanosilica samples at different calcination temperatures.
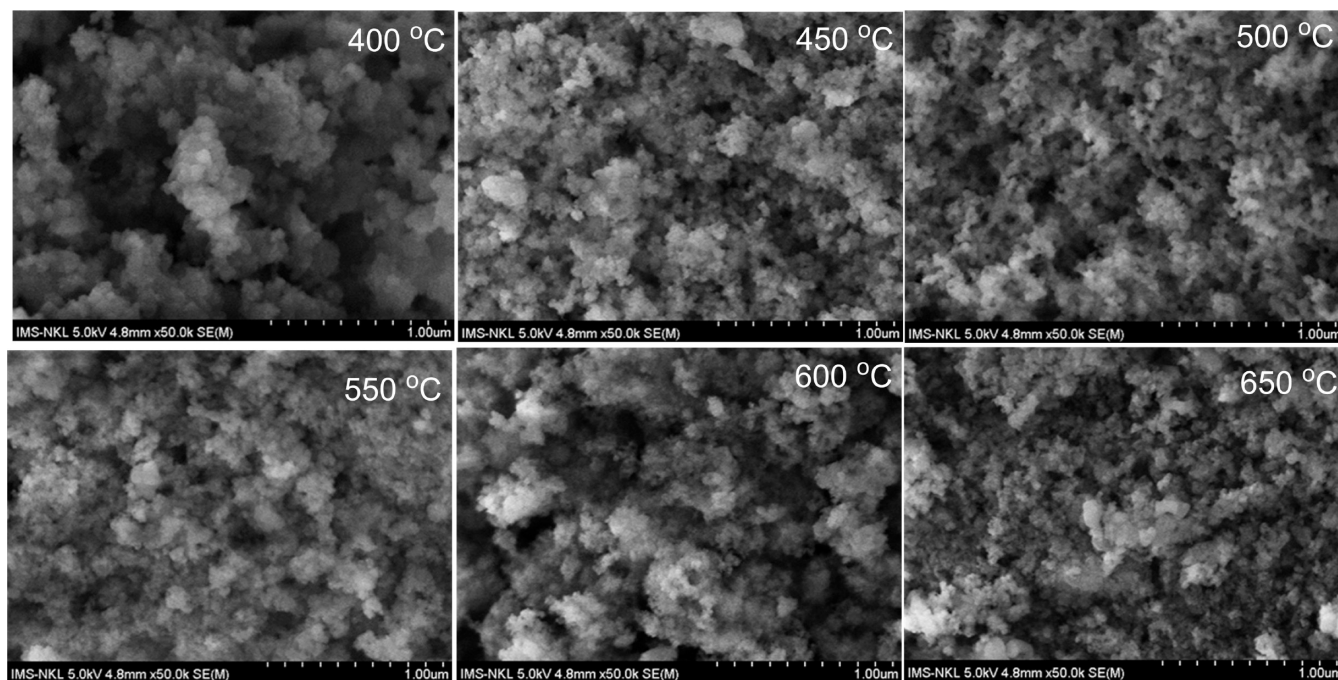
Figure 3. SEM images of nanosilica at different calcination temperatures.
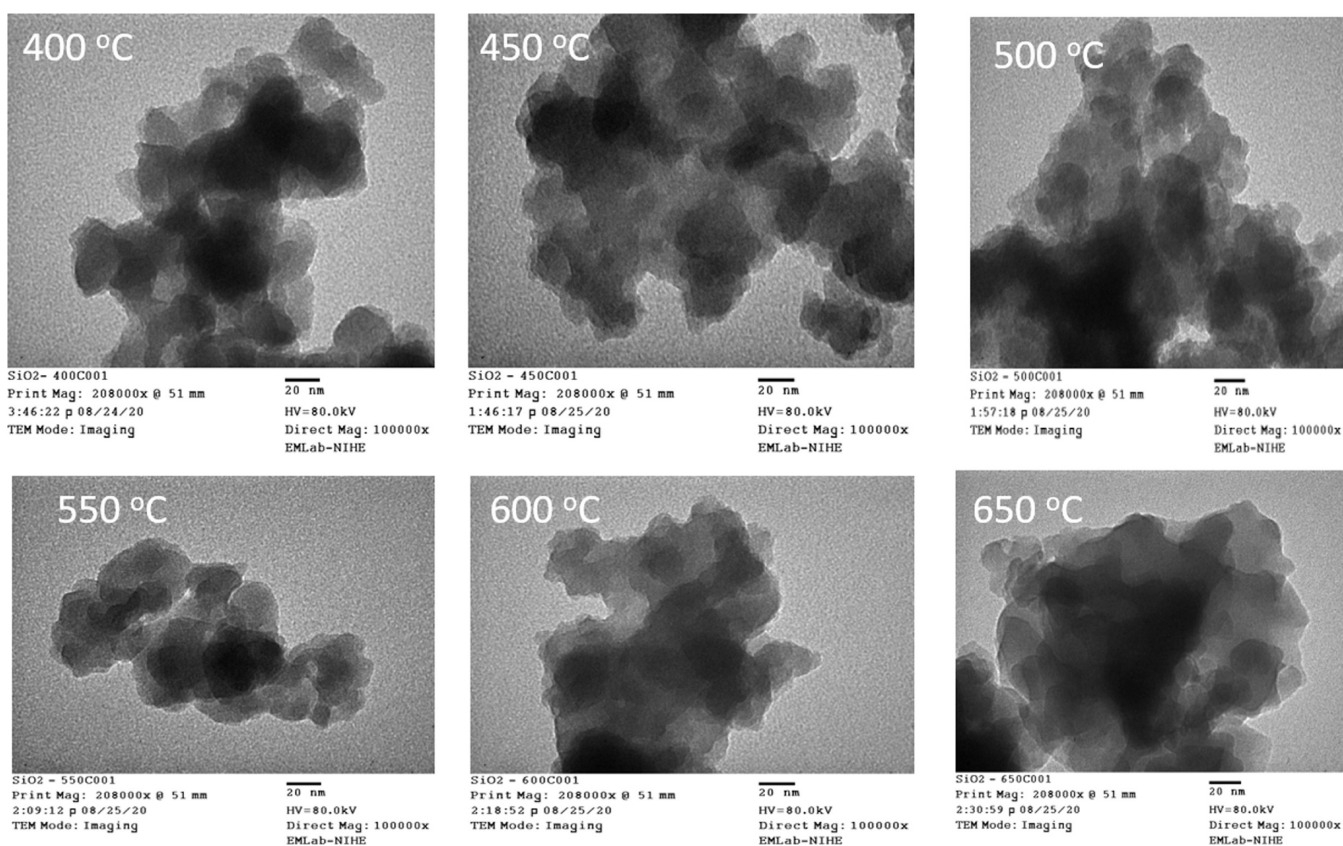

Figure 4. TEM images of nanosilica at different heating temperatures.

dissolution time, the experimental conditions were NaOH: 6N, particle size = 0.45 μm, and temperature: 180 °C. The results are shown in Figure 1b, revealing that maximum efficiency is reached at ~60 min. The experiments also showed that the decomposition efficiency increased with the increase in the concentration of NaOH, reaching a maximum at approximately

6N (Figure 1c). The temperature had an inflexion at ~180 °C (Figure 1d), above which the system became unstable due to softening of the reaction vessel (made of Teflon). Therefore, the NaOH concentration of 6N at 180 °C was fixed for further studies. Adding HCl to neutralize the solution led to condensation to form monosilicic acid, gradually agglomerat-
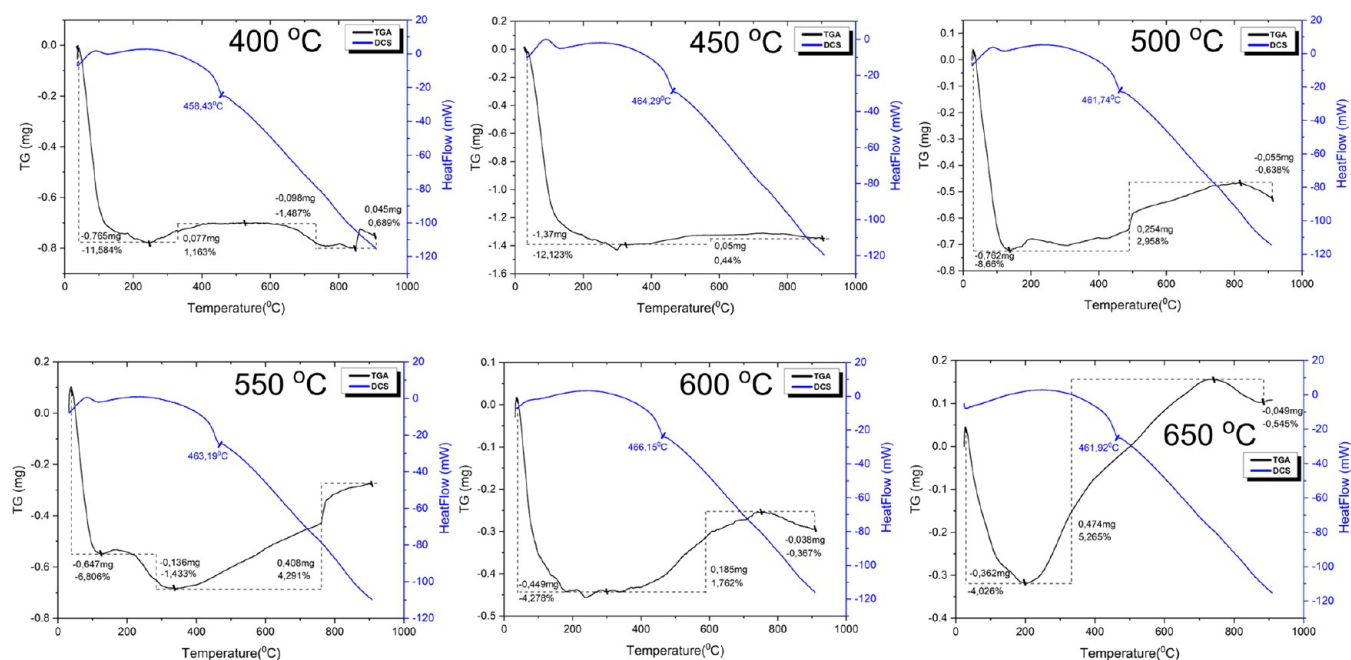
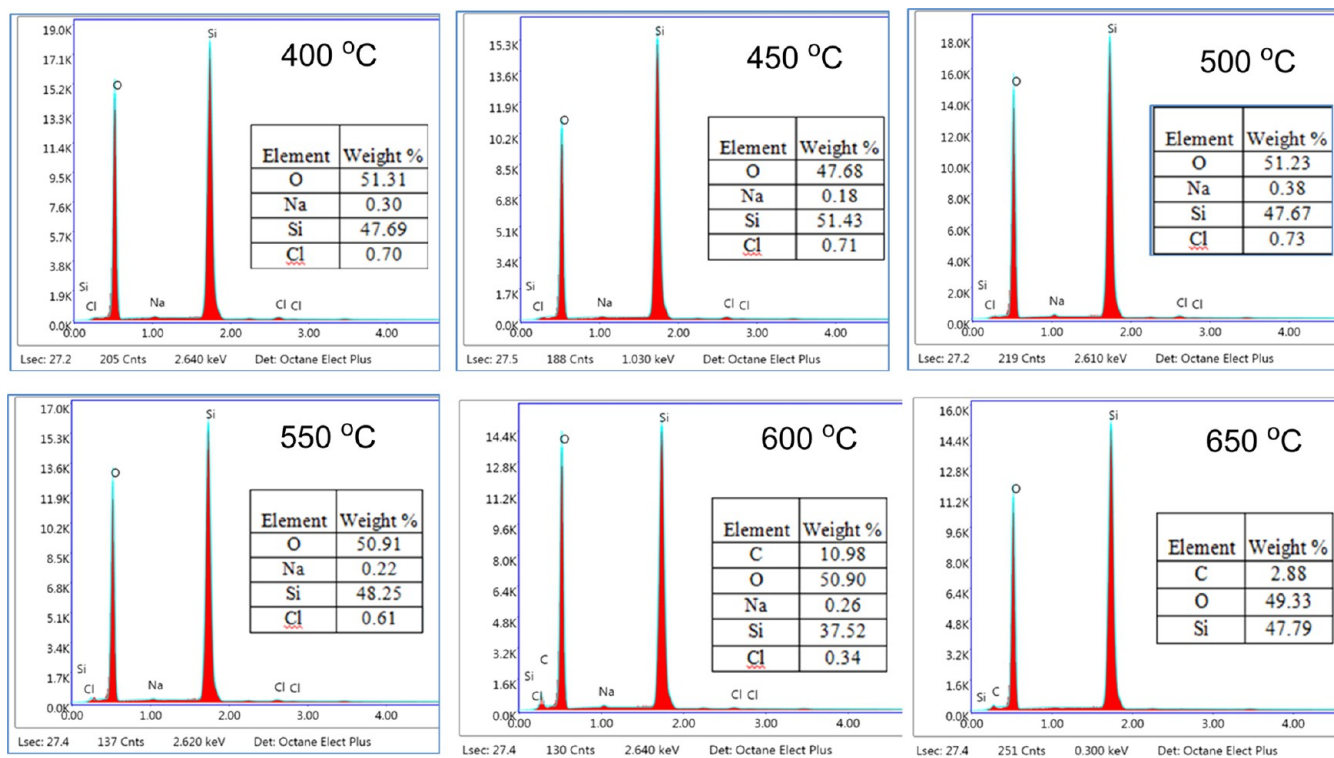**Figure 5.** Simultaneous thermal analysis diagram of TGA−DSC.

Figure 6. EDX spectra of the nanosilica at different calcination temperatures.

ing into a silica gel suspension. A large excess of hydrochloric acid was needed for neutralization with HCl 2−4N (143−127 mL), whereas for HCl 6−8N, the required volume was suitably low at 80−64 mL. Thus, HCN 6N was used for the synthesis. Thus, the optimization of conditions of the synthesis can be summarized as follows: sand particle size: 45 μm and NaOH (and HCl): 6N for 60 min at 180 °C. The protocol could be used to synthesize nanosilica from silica sand at a scale of 1 ton/h.

2.2. Characterization of the Synthesized Nanosilica.

2.2.1. X-ray Diffraction (XRD). The X-ray diffraction pattern of the samples at different temperatures (Figure 2) showed a characteristic peak of amorphous SiO_2 with a large half-spectral width at the position of about 21−22° (2θ) with weak intensity, indicating that the silica particles were small in size and mostly in the amorphous form. Additionally, the semispectral widths of the diffraction peaks of almost the same value confirmed that the synthesized silica nanoparticles of the samples were of approximately the same size at about
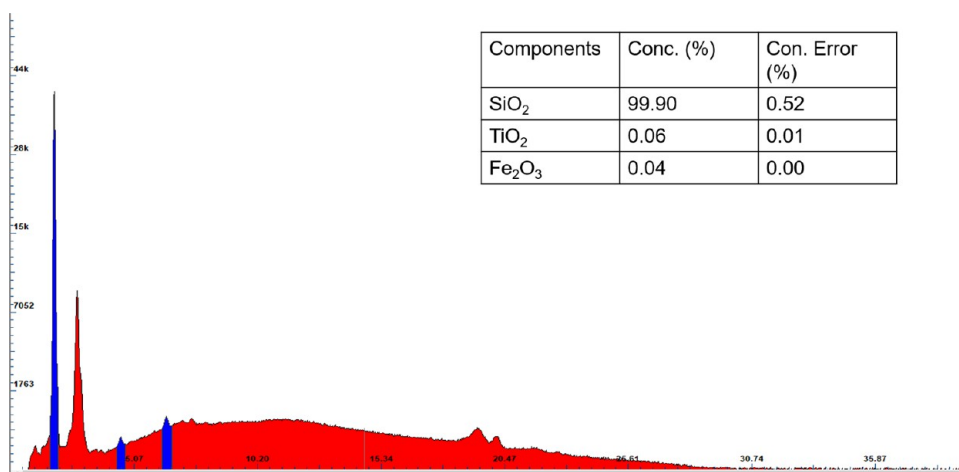
Components	Conc. (%)	Con. Error (%)
SiO_2	99.90	0.52
TiO_2	0.06	0.01
Fe_2O_3	0.04	0.00

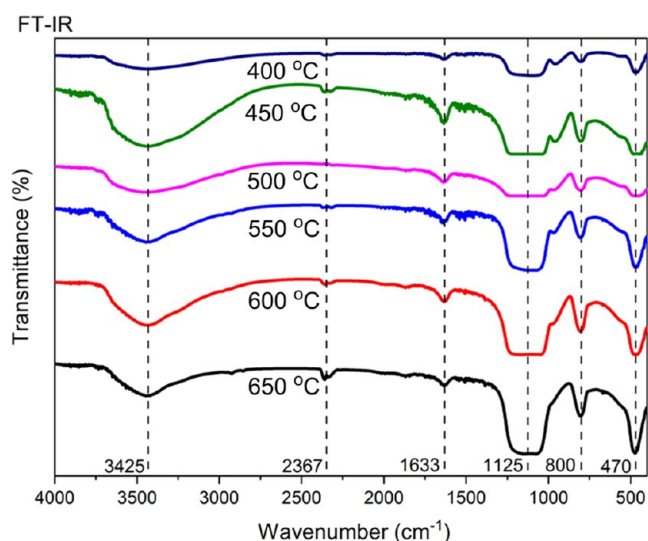**Figure 7.** XRF diagram of nanosilica.

Figure 8. FT-IR spectra of the nanosilica at different calcination temperatures.

26.8 nm (by the Scherrer equation[47]). This value was not affected by the calcination temperature.

2.2.2. Scanning Electron Microscopy (SEM). It can be seen from Figure 3 that the morphologies of the silica (SiO_2) particles of the above-mentioned samples were all granular with the same average size. The morphology suggested that the particles agglomerated and the clusters of particles were visibly porous that could be used as fertilizers.[7,10]

2.2.3. Transmission Electron Microscopy (TEM). To examine how the shape and size of the silica crystals change with increasing calcination temperature of the samples, these samples were further analyzed by TEM, and the results are presented in Figure 4 and Table S1. It was found that the particles were spherical in shape, with a fairly uniform size of about 16−23 nm, and tended to clump together to form a porous mass. It was also found that there was a decrease in the size of the nanosilica particles (from 26−37 to 16−24 nm) when increasing the sample heating temperature (400−650 °C). Thus, the most optimal temperature should be 650 °C.

2.2.4. Thermal Analysis Method (TGA−DSC). The TGA−differential scanning calorimetry (DSC) analysis (Figure 5) indicated that an average mass reduction effect of 7.912%

corresponded to an exothermic peak at a DSC of 100 °C and this mass reduction was due to the evaporation of water (present due to physical adsorption), whereas an average mass effect of 1.693% corresponded to an exothermic peak at a DSC of 200−700 °C and this mass reduction was due to the combustion of residual organic compounds. An average mass reduction effect of 0.686% corresponded to an exothermic peak at a DSC of 800−900 °C. At 600 °C, no physical or chemical changes were observed, indicating that SiO_2 oxide was formed.

2.2.5. Energy Dispersive X-ray Spectroscopy (EDX). From the EDX spectroscopy results (Figure 6), it was observed that the prepared SiO_2 nanosilica material, as expected, had the main atomic composition of Si and O at a ratio of approximately 1/2. In addition, the sample contained a little amount of C, which could be due to the incomplete combustion of organic contaminants during the sample heating process. The presence of Na and Cl elements was the result of neutralization with hydrochloric acid (HCl), which increasingly disappeared with increasing temperature from 400 to 650 °C. Therefore, when the sample was heated at a high temperature, i.e., 650 °C, the purity of the sample increased. Thus, the obtained SiO_2 materials were fairly pure.

2.2.6. X-ray Fluorescence (XRF). To assess the presence of trace contaminants in the sample, the synthesized nanosilica was analyzed by the XRF methods, and the results are presented in Figure 7 and Table S2.

In the XRF diagram, it can be observed that the main peak was SiO_2 (99.9%), whereas TiO_2 and Fe_2O_3 were also present in very low percentages at 0.06 and 0.04%, respectively. This indicated that the original sand ore contained TiO_2 and Fe_2O_3; however, the synthetic nanosilica was highly pure and dominated by the SiO_2 content.

2.2.7. Fourier Transform Infrared Spectroscopy (FT-IR). As shown in Figure 8, two peaks at 3425 and 1633 cm^{-1} characterized the valence and strain vibrations of the OH group of the free water molecules and the bonded silanol groups. It was found that the surface area of the particles increased in the 650 °C sample due to the adsorption of water on SiO_2. The peak at 2367 cm^{-1} with weak intensity corresponded to C−H oscillations, which meant that organic compounds were still not fully burnt. The three peaks at 1125, 800, and 470 cm^{-1} corresponded to the asymmetric valence vibration, the symmetric valence vibration, and the character-
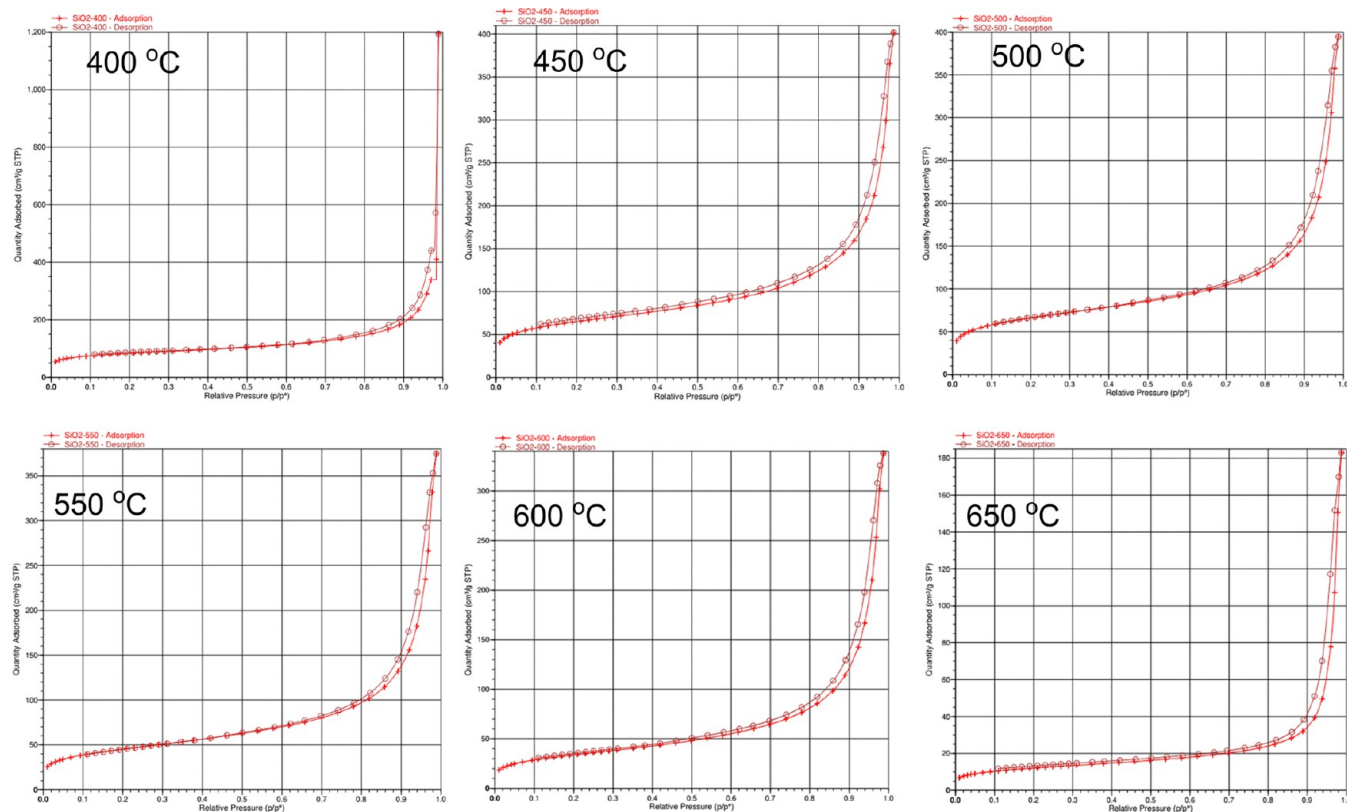
Figure 9. N$_2$ adsorption−desorption isotherms of nanosilica at different calcination temperatures.

Table 1. Results of Fertilizer Nanosilica on Corn Plants

| no.	targets	units	control (CT)	experiment (Exp)	compared with CT from Exp
1	sowing day		20/2/2021	20/2/2021	
	date of spraying nanosilica products		20/4/2021	18/4/2021	
2	flowering day (5−10%)		25/4/2021	23/4/2021	
3	flowering day (>90%)		8/5/2021	5/6/2021	
4	ripe day—harvest		20/2/2021	20/2/2021	
5	growth time	day	80−85	78−83	2
6	height of trees	cm	195	230	+35
7	blade length	cm	40	53	+13
8	tree size	cm	8−10	18−20	+10
9	number of fruits/tree	fruits	1−2	1−2	0
10	theoretical yield	ton/ha	45	45	0
11	real yield	ton/ha	43.5	56.3	+12.8
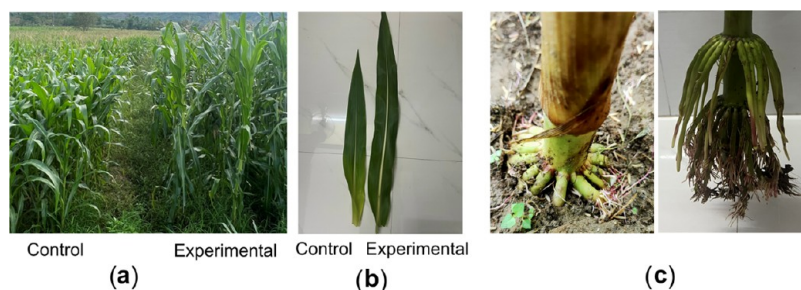
Figure 10. Control and experimental maize plants: (a) height of the plants; (b) blade length; and (c) root of experimental corn plants.

istic strain vibration of SiO$_2$ with the Si−O−Si bond, respectively. If the sample being tested had a Si−O bond, peaks will usually appear between 793 and 1050 cm^{-1}. For nanosized silica particles, the peak usually shifted to 1125 cm^{-1}. A peak at 800 cm^{-1} appeared to be a characteristic peak of the symmetric valence oscillation of the Si−O bond, whereas a peak at 470 cm^{-1} was attributed to the asymmetric strain oscillation of the Si−O bond.[33,48,49] The results of FT-IR

spectroscopy confirmed that the synthesized silica was pure and in the form of amorphous nanostructures.

2.2.8. N₂ Adsorption−Desorption Isotherm Method (BET). It was shown that the N_2 adsorption−desorption isotherms of the nanosilica (SiO_2) samples had a IV form, which was typical for materials with medium capillaries. The results showed that the samples were all similar in shape and size (Figures 9, S2 and Table S3). The presence of hysteresis showed capillary condensation and reflected the capillary geometry, whereas the hysteresis curve of H3-shaped materials was typical for materials with a structure containing many microcapillaries.

The BET adsorption isotherm of nanosilica (SiO_2) was typical for materials with medium capillary structures with low stability.[50] However, the Barrett−Joyner−Halenda (BJH) results showed that the surface area decreased and the capillary diameter increased with increasing calcination temperature. This could be explained by the fact that the higher the temperature, the faster the evaporation of water (due to physical adsorption) and the disintegration of the silanol functional groups (due to chemical adsorption). Therefore, the pressure exceeded the van der Waals forces that held the silica layers together, causing them to split and shatter. Therefore, the sample at 650 °C had an abnormally high capillary diameter. At such a high temperature, there was also the decomposition of NaCl, an intermediate compound in the synthesis of nanosilica. Compared to SiO_2 samples at other temperatures, the specific surface area and porous volume were greater at 400 °C. However, at 400 °C, the pore diameter of SiO_2 was smaller than that of any of the other samples. The capillary system for the sample consisted primarily of the average capillary, whereas the capillary widths of both substances ranged from 16 to 36 nm.

2.3. Testing Synthetic Nanosilica as a Fertilizer for Corn. The results of using synthetic nanosilica as a fertilizer for maize plants are shown in Table 1 and Figure 10. Monitoring data in the control and experimental areas (72 plants for each) revealed that the use of nanosilica on corn plants had a significant effect. In the test field, the blade length increased by 13 cm, the plant height increased by 35 cm on average, and the corn plants blossomed two days earlier as a result (Figure 10a,b). Additionally, corn plants with nanosilica inoculants were tougher and more durable than those without them, and root rot was not observed in the experimental maize plants (Figure 10c). Consequently, the yield per hectare increased to 12.8 tons. Thus, the data suggested that nanosilica had a favorable effect on maize, in good agreement with previous studies.[7,36,51]

3. CONCLUSIONS

Nanosilica particles were produced from silica sand using the sol−gel process with a high yield suitable for silica nanoparticle production on the industrial scale at one ton per hour. The structural analysis revealed that the synthesized materials were nanosized (16−37 nm) and highly pure (99.9% SiO_2). As a result of using nanosilica as a fertilizer for maize, the quantity and quality of the corn plants increased.

4. EXPERIMENTAL SECTION

4.1. Synthesis of Nanosilica. To a 250 mL beaker containing NaOH (6N, 100 mL), 60 g of the ground sand raw material (0.45 μm) was added with intensive stirring (Figure 11). The beaker was then placed in an oven at 180 °C for 8 h.
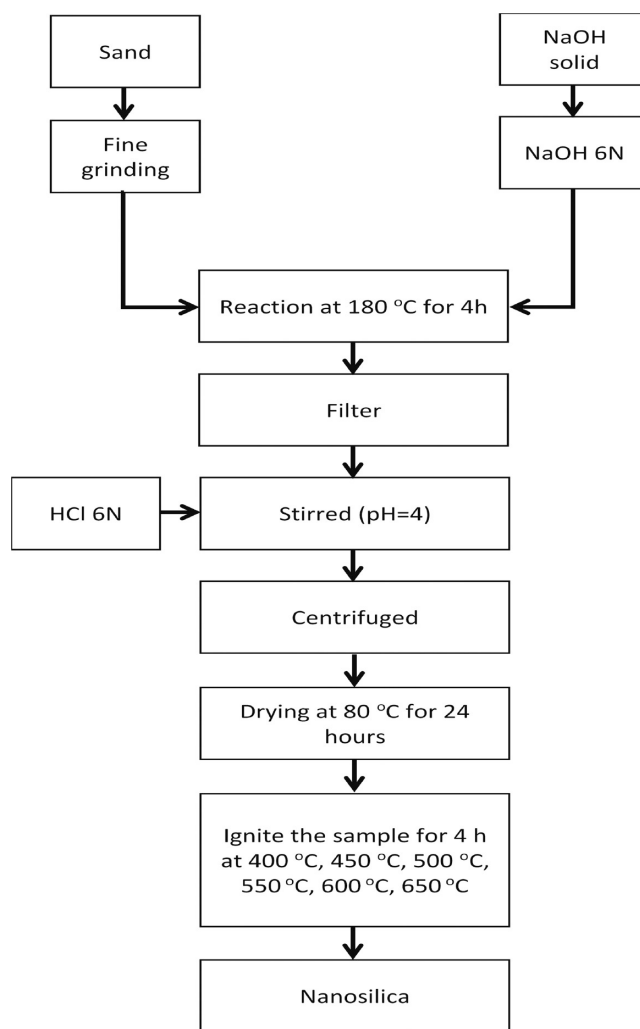

Figure 11. Process of synthesizing nanosilica from quartz sand.

The solvent was cooled to room temperature and then filtered to obtain a light-yellow sodium silicate solution. A HCl solution of 6N was slowly added to the mixture until the pH was reduced to ∼4, and a white precipitate was formed. The white precipitate solution was washed with distilled water several times until the residual acid was removed (pH = 7), and wet white powder was obtained. This material was dried at 80 °C for 24 h until completely dehydrated and then finely ground. The material was heated for 4 h at different temperatures of 400, 450, 500, 550, 600, and 650 °C to form the nanosilica (Figure 11).

4.2. Characterization. The prepared materials were analyzed using an X-ray diffractometer (XRD, Bruker, AXS D8) to investigate their microstructure. Material surfaces were characterized by scanning electronic microscopy (SEM) (JEOL JSM-6500F). Transmission electron microscopy (TEM) images of the synthesized materials were obtained using a JEOL TEM-2010F at an acceleration voltage of 200 kV. Infrared spectroscopy was performed on a 760 IR spectrometer (Nicolet). Energy dispersive X-ray spectroscopy was performed on an S-4800 spectrophotometer (EDX, Hitachi−Japan). The BET surface area of the materials was calculated, based on a Brunauer−Emmett−Teller isotherm determined by nitrogen adsorption and desorption at 77 K and

thermal analysis (Shimadzu DTA-50H thermal analyzer, Japan).

4.3. Testing Nanosilica Fertilizers for Maize Plants. The study was performed from July to November at the research farm of Quy Nhon University (13°46′0″ N, 109°14′10″E), Binh Dinh Province, Vietnam. The experimental location is used for annual maize production. It receives an average annual rainfall of 2617 mm and average annual minimum and maximum temperatures of 25 and 32 °C, respectively. Nanosilica at a concentration of 6.7 mg/L and a quantity of 300L/ha was used as a fertilizer (sprayed) twice at 15 and 45 days of age.

■ ASSOCIATED CONTENT

⑤ⁱ Supporting Information

The Supporting Information is available free of charge at https://pubs.acs.org/doi/10.1021/acsomega.2c05760.

> Particle size (TEM), XRD analysis, capillary distribution curve, and porous properties of the synthetic nanosilica (PDF)

■ AUTHOR INFORMATION

Corresponding Authors

Cao Van Hoang − *Quy Nhon University, Quy Nhon, Binh Dinh 590000, Vietnam*; Email: caovanhoang@qnu.edu.vn

Quan V. Vo − *The University of Danang - University of Technology and Education, Danang 550000, Vietnam;* ⑩ orcid.org/0000-0001-7189-9584; Email: vvquan@ute.udn.vn

Authors

Dang Nguyen Thoai − *Quy Nhon University, Quy Nhon, Binh Dinh 590000, Vietnam*

Nguyen Thi Dieu Cam − *Quy Nhon University, Quy Nhon, Binh Dinh 590000, Vietnam*

Tran Thi Thu Phuong − *Quy Nhon University, Quy Nhon, Binh Dinh 590000, Vietnam*

Nguyen Thi Lieu − *Quy Nhon University, Quy Nhon, Binh Dinh 590000, Vietnam*

Tran Thi Thu Hien − *Quy Nhon University, Quy Nhon, Binh Dinh 590000, Vietnam*

Dao Ngoc Nhiem − *Institute Materials Sciences, Vietnam Academy of Science and Technology, Ha Noi 100000, Vietnam*

Thanh-Dong Pham − *University of Natural Sciences - Vietnam National University, Ha Noi 100000, Vietnam*

Mai Huynh Thanh Tung − *Industrial University of Ho Chi Minh City, Ho Chi Minh City 700000, Vietnam*

Nguyen Thi To Tran − *Department of Agriculture & Rural Development, Quy Nhon, Binh Dinh 590000, Vietnam*

Adam Mechler − *Department of Biochemistry and Chemistry, La Trobe University, Victoria 3086, Australia;* ⑩ orcid.org/0000-0002-6428-6760

Complete contact information is available at:
https://pubs.acs.org/10.1021/acsomega.2c05760

Notes

The authors declare no competing financial interest.

■ REFERENCES

(1) Zainuri, M. Synthesis of SiO nanopowders containing quartz and cristobalite phases from silica sands. *Mater. Sci.* **2015**, *33*, 47−55.

(2) Anaia, G. C.; Freitas, P. A.; Suárez-Iha, M. E.; Rocha, F. R. Adsorption of 1-(2-thiazolylazo)-2-naphthol on amberlite XAD-7 and silica gel: isotherms and kinetic studies. *J. Braz. Chem. Soc.* **2014**, *25*, 648−657.

(3) Sprenger, S. Nanosilica-toughened epoxy resins. *Polymers* **2020**, *12*, 1777.

(4) Kim, S.-J.; Shin, B.-S.; Hong, J.-L.; Cho, W.-J.; Ha, C.-S. Reactive compatibilization of the PBT/EVA blend by maleic anhydride. *Polymer* **2001**, *42*, 4073−4080.

(5) Muthalvan, R. S.; Ravikumar, S.; Avudaiappan, S.; Amran, M.; Aepuru, R.; Vatin, N.; Fediuk, R. The Effect of Superabsorbent Polymer and Nano-Silica on the Properties of Blended Cement. *Crystals* **2021**, *11*, 1394.

(6) Sheng, H.; Chen, S. Plant silicon-cell wall complexes: Identification, model of covalent bond formation and biofunction. *Plant Physiol. Biochem.* **2020**, *155*, 13−19.

(7) Rastogi, A.; Tripathi, D. K.; Yadav, S.; Chauhan, D. K.; Živčák, M.; Ghorbanpour, M.; El-Sheery, N. I.; Brestic, M. Application of silicon nanoparticles in agriculture. *3 Biotech* **2019**, *9*, No. 90.

(8) Laing, M.; Gatarayiha, M.; Adandonon, A. *Silicon use for Pest Control in Agriculture: A Review*; SASTA, 2006; pp 278−286.

(9) El-Bendary, H.; El-Helaly, A. First record nanotechnology in agricultural: Silica nano-particles a potential new insecticide for pest control. *App. Sci. Rep.* **2013**, *4*, 241−246.

(10) Singh, S. P.; Endley, N. Fabrication of nano-silica from agricultural residue and their application. *Nanomater. Agric. For. Appl.* **2020**, 107−134.

(11) Mitchell, C.; Brennan, R. M.; Graham, J.; Karley, A. J. Plant defense against herbivorous pests: exploiting resistance and tolerance traits for sustainable crop protection. *Front. Plant Sci.* **2016**, *7*, No. 1132.

(12) Jones, L.; Ennos, A. R.; Turner, S. R. Cloning and characterization of irregular xylem4 (irx4): a severely lignin-deficient mutant of Arabidopsis. *Plant J.* **2001**, *26*, 205−216.

(13) Maxwell, F. G.; Jenkins, J. N.; Parrott, W. L. Resistance of plants to insects. *Adv. Agron.* **1972**, *24*, 187−265.

(14) Meena, V. D.; Dotaniya, M.; Coumar, V.; Rajendiran, S.; Ajay; Kundu, S.; Subba Rao, A. A case for silicon fertilization to improve crop yields in tropical soils. *Proc. Natl. Acad. Sci., India, Sect. B* **2014**, *84*, 505−518.

(15) Thabet, A. F.; Boraei, H. A.; Galal, O. A.; El-Samahy, M. F.; Mousa, K. M.; Zhang, Y. Z.; Tuda, M.; Helmy, E. A.; Wen, J.; Nozaki, T. Silica nanoparticles as pesticide against insects of different feeding types and their non-target attraction of predators. *Sci. Rep.* **2021**, *11*, No. 14484.

(16) Wu, S.-H.; Mou, C.-Y.; Lin, H.-P. Synthesis of mesoporous silica nanoparticles. *Chem. Soc. Rev.* **2013**, *42*, 3862−3875.

(17) Sanyal, S.; De Datta, S. Chemistry of phosphorus transformations in soil. *Adv. Soil Sci.* **1991**, 1−120.

(18) Borawska-Jarmułowicz, B.; Mastalerczuk, G.; Janicka, M.; Wróbel, B. Effect of silicon-containing fertilizers on the nutritional value of grass−legume mixtures on temporary grasslands. *Agriculture* **2022**, *12*, 145.

(19) Savant, N.; Snyder, G.; Datnoff, L. Silicon management and sustainable rice production. *Adv. Agron.* **1996**, *58*, 151−199.

(20) Liang, Y.; Si, J.; Römheld, V. Silicon uptake and transport is an active process in Cucumis sativus. *New Phytol.* **2005**, *167*, 797−804.

(21) Ayres, A. S. Calcium silicate slag as a growth stimulant for sugarcane on low-silicon soils. *Soil Sci.* **1966**, *101*, 216−227.

(22) Datnoff, L. E.; Snyder, G.; Deren, C. Influence of silicon fertilizer grades on blast and brown spot development and on rice yields. *Plant Dis.* 1992, 76, 1011−1013.

(23) Epstein, E. Silicon. *Annu. Rev. Plant Physiol. Plant Mol. Biol.* 1999, 50, 641−664.

(24) Rodrigues, F.; Datnoff, L.; Korndörfer, G.; Seebold, K.; Rush, M. Effect of silicon and host resistance on sheath blight development in rice. *Plant Dis.* 2001, 85, 827−832.

(25) Schlomach, J.; Kind, M. Investigations on the semi-batch precipitation of silica. *J. Colloid Interface Sci.* 2004, 277, 316−326.

(26) Takahashi, E. Uptake mode and physiological functions of silica. *Sci. Rice Plant* 1995, 2, 58−71.

(27) Ram, P.; Kumar, V.; Prasad, K. S. Nanotechnology in sustainable agriculture: present concerns and future aspects. *Afr. J. Biotechnol.* 2014, 13, 705−713.

(28) Sergent, J.-A.; Paget, V.; Chevillard, S. Toxicity and genotoxicity of nano-SiO2 on human epithelial intestinal HT-29 cell line. *Ann. Occup. Hyg.* 2012, 56, 622−630.

(29) Rameshaiah, G.; Pallavi, J.; Shabnam, S. Nano fertilizers and nano sensors−an attempt for developing smart agriculture. *Int. J. Eng. Res. Gen. Sci.* 2015, 3, 314−320.

(30) Toksha, B.; Sonawale, V. A. M.; Vanarase, A.; Bornare, D.; Tonde, S.; Hazra, C.; Kundu, D.; Satdive, A.; Tayde, S.; Chatterjee, A. Nanofertilizers: A review on synthesis and impact of their use on crop yield and environment. *Environ. Technol. Innov.* 2021, 24, No. 101986.

(31) Mor, S.; Manchanda, C. K.; Kansal, S. K.; Ravindra, K. Nanosilica extraction from processed agricultural residue using green technology. *J. Cleaner Prod.* 2017, 143, 1284−1290.

(32) Ismail, A.; Saputri, L.; Dwiatmoko, A.; Susanto, B.; Nasikin, M. A facile approach to synthesis of silica nanoparticles from silica sand and their application as superhydrophobic material. *J. Asian Ceram. Soc.* 2021, 9, 665−672.

(33) Rafiee, E.; Shahebrahimi, S.; Feyzi, M.; Shaterzadeh, M. Optimization of synthesis and characterization of nanosilica produced from rice husk (a common waste material). *Int. Nano Lett.* 2012, 2, 1−8.

(34) Thuc, C. N. H.; Thuc, H. H. Synthesis of silica nanoparticles from Vietnamese rice husk by sol−gel method. *Nanoscale Res. Lett.* 2013, 8, No. 58.

(35) Sankar, S.; Sharma, S. K.; Kaur, N.; Lee, B.; Kim, D. Y.; Lee, S.; Jung, H. Biogenerated silica nanoparticles synthesized from sticky, red, and brown rice husk ashes by a chemical method. *Ceram. Int.* 2016, 42, 4875−4885.

(36) Naskar, M. K.; Kundu, D.; Chatterjee, M. Coral-like hydroxy sodalite particles from rice husk ash as silica source. *Mater. Lett.* 2011, 65, 3408−3410.

(37) Rossi, L. M.; Shi, L.; Quina, F. H.; Rosenzweig, Z. Stöber synthesis of monodispersed luminescent silica nanoparticles for bioanalytical assays. *Langmuir* 2005, 21, 4277−4280.

(38) Munasir; Sulton, A.; Triwikantoro; Zainuri, M.; Darminto In *Synthesis of Slica Nanopowder Produced from Indonesian Natural Sand via Alkalifussion Route*, AIP Conf. Proc.; American Institute of Physics, 2013; pp 28−31.

(39) Supardi, Z. A. I.; Nisa, Z.; Kusumawati, D. H.; Putri, N. P.; Taufiq, A.; Hidayat, N. Phase transition of SiO2 nanoparticles prepared from natural sand: the calcination temperature effect. *J. Phys.: Conf. Ser.* 2018, No. 012025.

(40) Arunmetha, S.; Karthik, A.; Srither, S. R.; Vinoth, M.; Suriyaprabha, R.; Manivasakan, P.; Rajendran, V. Size-dependent physicochemical properties of mesoporous nanosilica produced from natural quartz sand using three different methods. *RSC Adv.* 2015, 5, 47390−47397.

(41) Kadhim, R. A.; Mohammed, A. A.; Hussein, H. M. Synthesis and preparation of Nano-silica particles from Iraqi western region silica sand via SOL-GEL method. *J. Phys.: Conf. Ser.* 2021, No. 012071.

(42) Razak, N. A. A.; Othman, N. H.; Shayuti, M. S. M.; Jumahat, A.; Sapiai, N.; Lau, W. J. Agricultural and industrial waste-derived mesoporous silica nanoparticles: A review on chemical synthesis route. *J. Environ. Chem. Eng.* 2022, No. 107322.

(43) Osman, N. S.; Sapawe, N. Waste material as an alternative source of silica precursor in silica nanoparticle synthesis−a review. *Mater. Today: Proc.* 2019, 19, 1267−1272.

(44) Wahyudi, A.; Amalia, D.; Sariman, S. Preparation of nano silica from silica sand through alkali fusion process. *Indones. Min. J.* 2013, 16, 149−153.

(45) Hajimohammadi, A.; van Deventer, J. S. Dissolution behaviour of source materials for synthesis of geopolymer binders: A kinetic approach. *Int. J. Miner. Process.* 2016, 153, 80−86.

(46) Niibori, Y.; Kunita, M.; Tochiyama, O.; Chida, T. Dissolution rates of amorphous silica in highly alkaline solution. *J. Nucl. Sci. Technol.* 2000, 37, 349−357.

(47) Muniz, F. T. L.; Miranda, M. R.; Morilla dos Santos, C.; Sasaki, J. M. The Scherrer equation and the dynamical theory of X-ray diffraction. *Acta Crystallogr., Sect. A: Found. Adv.* 2016, 72, 385−390.

(48) Yuvakkumar, R.; Elango, V.; Rajendran, V.; Kannan, N. High-purity nano silica powder from rice husk using a simple chemical method. *J. Exp. Nanosci.* 2014, 9, 272−281.

(49) Mehravar, M.; Mirjalili, B. B. F.; Babaei, E.; Bamoniri, A. Nano-SiO2/DBN: an efficacious and reusable catalyst for one-pot synthesis of tetrahydrobenzo [b] pyran derivatives. *BMC Chem.* 2021, 15, No. 34.

(50) Donohue, M. D.; Aranovich, G. A new classification of isotherms for Gibbs adsorption of gases on solids. *Fluid Phase Equilib.* 1999, 158−160, 557−563.

(51) Cuong, T. X.; Ullah, H.; Datta, A.; Hanh, T. C. Effects of silicon-based fertilizer on growth, yield and nutrient uptake of rice in tropical zone of Vietnam. *Rice Sci.* 2017, 24, 283−290.